Effect of Core and Face Sheet Anisotropy on the Natural Frequencies of Sandwich Shells with Composite Faces

Jörg Hohe[1]

[1]Fraunhofer-Institut für Werkstoffmechanik IWM, 79108 Freiburg, Germany

Abstract The objective of the present study is the analysis of the effect of core and face sheet anisotropy on the natural frequencies of plane and doubly curved sandwich structures with laminated composite face sheets and an anisotropic core. For the analysis, a higher-order sandwich shell theory is adopted. For the special case of a sandwich shell with rectangular projection, an analytical solution is obtained by means of an extended Galerkin procedure. Assuming a harmonic time-dependent response, the problem is transformed into an eigenvalue problem, which can be solved in a numerically rather efficient manner. The numerical scheme is applied to an analysis of the effect of the face sheet anisotropy induced by fibre angle variations in laminated face sheets consisting of unidirectionally infinite fibre reinforced carbon epoxy plies. Further anisotropy effects derive from the use of honeycomb cores with anisotropy transverse shear moduli. It is observed that anisotropy of core and face sheets may have distinct effects on the lower natural frequencies.

Keywords Sandwich Structures, Composite Face Sheets, Anisotropy, Analytical Model, Natural Frequencies

1. Introduction

Structural sandwich panels are important elements in modern lightweight structures. The typical sandwich panel is a layered structure according to Figure 1. It consists of three principal layers where two high-density face sheets are adhesively bonded to a low density core. The face sheets carry all in-plane and bending loads whereas the core keeps the face sheets at their desired distance and transmits the transverse normal and shear loads. The advantage of the sandwich principle is that plates and shells with high bending stiffness may be constructed at an extremely low specific weight (Vinson [13], Zenkert [16]).

Typical face sheet materials are thin metal sheets or – especially in high performance applications – composite laminates consisting of unidirectionally infinite carbon or glass fibre reinforced plastic plies. Depending on the stacking sequence of the laminates, the face sheets may feature a distinct anisotropy which may be exploited towards the design of tailored structures with optimized properties complying with any kind of prescribed structural requirement. The core is usually made from a weak, low density material such as balsa wood, solid foam or a two-dimensional honeycomb type cellular structure. Especially honeycomb cores may feature a distinct anisotropy since their transverse shear moduli with respect to the two in-plane directions are usually not identical (Gibson and Ashby [3]).

The dynamic response and vibration of sandwich structures is a challenging problem since not only the external geometry of the plate or shell but also the anisotropy of core and face sheets may affect the response of the structure. Following the pioneering experimental study by Raville and Ueng [11] in 1967, increasing interest has been directed to the vibration of sandwich plates and shells especially during the past two decades. Bardell et al. [1] have analysed the free vibration of plane isotropic sandwich plates with different external shapes using the finite element method. The free vibration of sandwich plates with laminated anisotropic face sheets has been investigated by Zhou and Li [17] as well as by Kant and Swaminathan [8] using different quasi-analytical models. Yuan and Dawe [14] employed the spline finite strip method to the analysis of the eigenmodes of plane sandwich plates with laminated composite faces. In a later study, this approach has been extended to the problem of plane sandwich plates with stiffeners on one side (Yuan and Dawe [15]). Since the deformation behaviour of

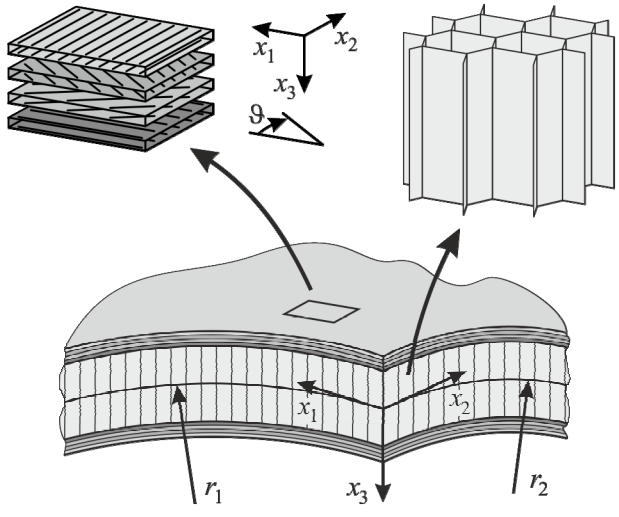

Figure 1. Doubly Curved Sandwich Shell.

sandwich structures with soft cores in general is much more complex than the response of sandwich structures with stiff, transversely incompressible cores, a number of studies use higher-order sandwich models for the analysis of the free vibration problem. Sokolinsky et al. [12] have analysed the lower natural frequencies of straight sandwich beams with isotropic core and faces using Frostig's soft core sandwich beam model. More recently, a study on the effects of the transverse core flexibility on the vibrational response of two-dimensional sandwich plates with quasi-isotropic core and faces using an extended flexible core model has been provided by Frostig and Thomsen [2]. Meunier and Shenoi [9] have been concerned with a higher-order model accounting for damping effects whereas Nayak et al. [10] employed Reddy's higher-order model. Both studies are concerned with plane sandwich plates. However, in contrast to the previous studies, anisotropy effects are included for both, the core and the face sheets. In a similar manner, Hause and Librescu [4] analysed the vibration of anisotropic sandwich plates based on an earlier version of the present sandwich shell theory (Hohe and Librescu [5], [6]). Again, the study is restricted to plane sandwich plates. In a preceding study by the present author (Hohe et al. [7]) on the transient response of sandwich structures during and after rapid loading, the effect of curvature has been included. Nevertheless, the study is again restricted to sandwich panels made from isotropic materials.

Objective of the present contribution is an analysis of the effects of the anisotropy of core and face sheets on the lower natural frequencies of plane sandwich plates as well as cylindrical and doubly curved sandwich shells. Special interest is directed to interaction effects between the external shape and the local core and face sheet anisotropy. The analysis is based on a general model for curved sandwich shells presented earlier by the present author (Hohe and Librescu [5], [6]). The original nonlinear model is simplified and adapted to the requirements of the present linear problem. Based on an extended Galerkin procedure, an analytical displacement solution is derived. Assuming harmonic oscillations as the only relevant type of displacement, an eigenvalue problem for the natural frequencies in different eigenmodes is obtained. The problem is solved numerically by means of the Newton-Raphson method. In parametric studies the effect of core and face sheet anisotropy on the lower natural frequencies for a sandwich shell with carbon epoxy face sheets and honeycomb core is studied. It is observed that the core and face sheet anisotropy may have different effects on the different eigenfrequencies.

2. Sandwich Shell Model

2.1 Basic Assumptions

For the analyses of the present study, the general shell model for shallow sandwich shells presented earlier (Hohe and Librescu [5], [6]) is adopted. The model is re-formulated into a simplified version complying with the requirements of the present problem.

Consider a plane or curved sandwich shell according to Figure 1. The face sheets are assumed to consist of composite laminates with constant thickness t^f. The core thickness t^c is also uniform but much larger than the face sheet thickness t^f. The sandwich panel is assumed to be doubly curved with radii of curvature r_i which are much larger than the panel thickness so that the conditions of shallow shell theory are satisfied (Figure 1). For the analysis of the sandwich structure, a local Cartesian system x_i is introduced, where x_1 and x_2 are the in-plane direction whereas x_3 is the transverse normal direction.

Both, the core and the face sheets are assumed to be linear elastic but anisotropic. For the core, the effective material parameters are assumed to be known directly whereas the face sheet material response is assumed to be given in terms of the laminate stiffness matrix of the classical laminate theory. Since the deflections in the free vibration problem in general are small, a geometrically linear analysis is sufficient. No geometric imperfections are considered, although both features are included in the original model (Hohe and Librescu [5], [6]).

2.2 Kinematic relations

For a projection of the shell deformation behaviour onto the reference surface, the three dimensional displacements are expanded into a power series in terms of x_3. Since the material response and the thickness of core and face sheets are rather different, an effective multilayer model is adopted, treating the three principal layers (core, top and bottom face sheet) separately.

Since the face sheets are thin, the Kirchhoff-Love model is adopted for the faces. Thus, the face sheet displacements are given by

$$\begin{aligned} u_1^{\mathrm{t}} &= u_1^{\mathrm{a}} + u_1^{\mathrm{d}} - \left(x_3 + \tfrac{t+t^{\mathrm{f}}}{2}\right)\left(u_{3,1}^{\mathrm{a}} + u_{3,1}^{\mathrm{d}}\right) \\ u_2^{\mathrm{t}} &= u_2^{\mathrm{a}} + u_2^{\mathrm{d}} - \left(x_3 + \tfrac{t+t^{\mathrm{f}}}{2}\right)\left(u_{3,2}^{\mathrm{a}} + u_{3,2}^{\mathrm{d}}\right) \\ u_3^{\mathrm{t}} &= u_3^{\mathrm{a}} + u_3^{\mathrm{d}} \end{aligned} \tag{1}$$

for the top face and

$$\begin{aligned} u_1^{\mathrm{b}} &= u_1^{\mathrm{a}} - u_1^{\mathrm{d}} - \left(x_3 - \tfrac{t+t^{\mathrm{f}}}{2}\right)\left(u_{3,1}^{\mathrm{a}} - u_{3,1}^{\mathrm{d}}\right) \\ u_2^{\mathrm{b}} &= u_2^{\mathrm{a}} - u_2^{\mathrm{d}} - \left(x_3 - \tfrac{t+t^{\mathrm{f}}}{2}\right)\left(u_{3,2}^{\mathrm{a}} - u_{3,2}^{\mathrm{d}}\right) \\ u_3^{\mathrm{b}} &= u_3^{\mathrm{a}} - u_3^{\mathrm{d}} \end{aligned} \tag{2}$$

for the bottom face, where

$$\begin{aligned} u_i^{\mathrm{a}} &= \tfrac{1}{2}\left(u_i^{\mathrm{t}} + u_i^{\mathrm{b}}\right) \\ u_i^{\mathrm{d}} &= \tfrac{1}{2}\left(u_i^{\mathrm{t}} - u_i^{\mathrm{b}}\right) \end{aligned} \tag{3}$$

are the average and the deviation from the average of the face sheet mid-surface face sheet displacements u_i^{t} and u_i^{b}.

For the core, a higher order power series expansion of the displacements is employed in order to account for the transverse compressibility of the central layer in the weak core limit. Considering the compatibility requirements of the core and face sheet displacements at the interfaces at $x_3 = \pm t^c/2$, the core displacements read

$$\begin{aligned} u_1^{\mathrm{c}} &= u_1^{\mathrm{a}} - \tfrac{t^{\mathrm{f}}}{2} u_{3,1}^{\mathrm{d}} - \tfrac{2}{t^{\mathrm{c}}} x_3 u_1^{\mathrm{d}} + \tfrac{t^{\mathrm{f}}}{t^{\mathrm{c}}} x_3 u_{3,1}^{\mathrm{a}} + \left(\left(\tfrac{2x_3}{t^{\mathrm{c}}}\right)^2 - 1\right)\Omega_1^{\mathrm{c}} \\ u_2^{\mathrm{c}} &= u_2^{\mathrm{a}} - \tfrac{t^{\mathrm{f}}}{2} u_{3,2}^{\mathrm{d}} - \tfrac{2}{t^{\mathrm{c}}} x_3 u_2^{\mathrm{d}} + \tfrac{t^{\mathrm{f}}}{t^{\mathrm{c}}} x_3 u_{3,2}^{\mathrm{a}} + \left(\left(\tfrac{2x_3}{t^{\mathrm{c}}}\right)^2 - 1\right)\Omega_2^{\mathrm{c}} \\ u_3^{\mathrm{c}} &= u_3^{\mathrm{a}} - \tfrac{2}{t^{\mathrm{c}}} x_3 u_3^{\mathrm{d}} \end{aligned} \tag{4}$$

where Ω_i^c are additional displacement functions. These additional degrees of freedom describe a quadratic displacement through the layer thickness in addition to the mid-surface displacements as well as the rotations and thus account for the warping of the core.

From Equations (1) to (4), the strains for the three principal layers are obtained by substituting the expressions into the geometrically linear kinematic relation. Under the assumption of the shallow shell limit, the strains

$$\begin{aligned}
\varepsilon_{11} &= u_{1,1} - \tfrac{1}{r_1} u_3 \\
\varepsilon_{22} &= u_{2,2} - \tfrac{1}{r_2} u_3 \\
\varepsilon_{33} &= u_{3,3} \\
\varepsilon_{23} &= \tfrac{1}{2}\left(u_{2,3} + u_{3,2}\right) \\
\varepsilon_{13} &= \tfrac{1}{2}\left(u_{1,3} + u_{3,1}\right) \\
\varepsilon_{12} &= \tfrac{1}{2}\left(u_{1,2} + u_{2,1}\right)
\end{aligned} \tag{5}$$

are obtained for the three principal layers.

2.3 Equations of Motion

In the next step, equations of motion have to be determined, which are consistent with the assumptions made in the kinematic considerations. A natural manner to determine an inherently consistent shell theory is the use of Hamilton's variational principle

$$\int_{t^0}^{t^1} (\delta U - \delta W - \delta T)\,\mathrm{d}t = 0 \tag{6}$$

where δU, δW and δT are the variations of the strain energy, the work by the external loads and the kinetic energy respectively whereas $[t^0, t^1]$ is an arbitrary time increment.

In the context of the present multilayer model and the corresponding simplifying assumptions, the variation of the strain energy is defined by

$$\delta U = \int_A \left(\int_{-t^f - \frac{t^c}{2}}^{-\frac{t^c}{2}} \sigma_{\alpha\beta}^{\mathrm{t}} \delta\varepsilon_{\alpha\beta}^{\mathrm{t}}\,\mathrm{d}x_3 + \int_{-\frac{t^c}{2}}^{\frac{t^c}{2}} \sigma_{i3}^{\mathrm{c}} \delta\varepsilon_{i3}^{\mathrm{c}}\,\mathrm{d}x_3 + \int_{\frac{t^c}{2}}^{\frac{t^c}{2}+t^f} \sigma_{\alpha\beta}^{\mathrm{b}} \delta\varepsilon_{\alpha\beta}^{\mathrm{b}}\,\mathrm{d}x_3 \right) \mathrm{d}A \tag{7}$$

where A is the reference surface area of the structure under consideration. As usual, $\alpha, \beta = 1, 2$ whereas $i, j = 1, 2, 3$. The work of the in-plane stresses within the core layer is neglected.

Assuming that only transverse normal distributed loads $q_3^{\mathrm{t}*}$ and $q_3^{\mathrm{b}*}$ act on the surfaces of the top and bottom face sheets, the variation of the work by the external loads read

$$\begin{aligned}
\delta W = &\int_A \left(q_3^{\mathrm{t}*} \delta u_3^{\mathrm{t}} + q_3^{\mathrm{b}*} \delta u_3^{\mathrm{b}} \right) \mathrm{d}A \\
&+ \int_{x_t} \left(\int_{-t^f - \frac{t^c}{2}}^{-\frac{t^c}{2}} \sigma_{n\alpha}^{\mathrm{t}} \delta u_\alpha^{\mathrm{t}}\,\mathrm{d}x_3 + \int_{-\frac{t^c}{2}}^{\frac{t^c}{2}} \sigma_{n3}^{\mathrm{c}} \delta u_3^{\mathrm{c}}\,\mathrm{d}x_3 + \int_{\frac{t^c}{2}}^{\frac{t^c}{2}+t^f} \sigma_{n\alpha}^{\mathrm{b}} \delta u_\alpha^{\mathrm{b}}\,\mathrm{d}x_3 \right) \mathrm{d}x_t
\end{aligned} \tag{8}$$

where x_n and x_t are the normal and tangential direction of a local Cartesian coordinate system along the external boundary of the sandwich shell where the prescribed stresses σ_{ij}^* are acting.

For the kinetic energy, an additional simplification is introduced by neglecting all in-plane and rotational inertia effects since in the free vibration problem, the transverse motion within the x_3-direction is the dominant mode of deflection. With this assumption and the mass densities ρ^{c} and ρ^{f} for the core and the face sheets respectively, the variation of the kinetic energy becomes

$$\delta T = \int_A \left(\int_{-t^f - \frac{t^c}{2}}^{-\frac{t^c}{2}} -\rho^{\mathrm{f}} \ddot{u}_3^{\mathrm{t}} \delta u_3^{\mathrm{t}}\,\mathrm{d}x_3 - \int_{-\frac{t^c}{2}}^{\frac{t^c}{2}} \rho^{\mathrm{c}} \ddot{u}_3^{\mathrm{c}} \delta u_3^{\mathrm{c}}\,\mathrm{d}x_3 - \int_{\frac{t^c}{2}}^{\frac{t^c}{2}+t^f} \rho^{\mathrm{f}} \ddot{u}_3^{\mathrm{b}} \delta u_3^{\mathrm{b}}\,\mathrm{d}x_3 \right) \mathrm{d}A. \tag{9}$$

Determining the virtual strains $\delta\varepsilon_{ij}$ for the three principal layers of the sandwich structure using Equation (5) and substituting the result together with the shell kinematics (1) to (4) into Hamilton's principle (6) with the variations of the strain energy, work by the external loads and kinetic energy according to Equations (7) to (9) results in a lengthy variational expression. Within this expression, the stresses and the explicit powers of x_3 are the only terms which depend on the transverse direction. Hence the stress resultants for the three principal layers

$$\begin{aligned}
\left\{N_{\alpha\beta}^{\mathrm{t}}, M_{\alpha\beta}^{\mathrm{t}}\right\} &= \int_{-t^f - \frac{t^c}{2}}^{-\frac{t^c}{2}} \sigma_{\alpha\beta}^{\mathrm{t}} \left\{1, \left(x_3 + \tfrac{t^c + t^f}{2}\right)\right\} \mathrm{d}x_3 \\
\left\{N_{i3}^{\mathrm{c}}, M_{i3}^{\mathrm{c}}\right\} &= \int_{-t^f - \frac{t^c}{2}}^{-\frac{t^c}{2}} \sigma_{\alpha\beta}^{\mathrm{c}} \left\{1, x_3\right\} \mathrm{d}x_3 \\
\left\{N_{\alpha\beta}^{\mathrm{b}}, M_{\alpha\beta}^{\mathrm{b}}\right\} &= \int_{\frac{t^c}{2}}^{t^f + \frac{t^c}{2}} \sigma_{\alpha\beta}^{\mathrm{b}} \left\{1, \left(x_3 - \tfrac{t^c + t^f}{2}\right)\right\} \mathrm{d}x_3
\end{aligned} \tag{10}$$

with the alternative definition

$$\begin{aligned}
\left\{N_{\alpha\beta}^{\mathrm{a}}, M_{\alpha\beta}^{\mathrm{a}}\right\} &= \tfrac{1}{2}\left(\left\{N_{\alpha\beta}^{\mathrm{t}}, M_{\alpha\beta}^{\mathrm{t}}\right\} + \left\{N_{\alpha\beta}^{\mathrm{b}}, M_{\alpha\beta}^{\mathrm{b}}\right\}\right) \\
\left\{N_{\alpha\beta}^{\mathrm{d}}, M_{\alpha\beta}^{\mathrm{d}}\right\} &= \tfrac{1}{2}\left(\left\{N_{\alpha\beta}^{\mathrm{t}}, M_{\alpha\beta}^{\mathrm{t}}\right\} - \left\{N_{\alpha\beta}^{\mathrm{b}}, M_{\alpha\beta}^{\mathrm{b}}\right\}\right)
\end{aligned} \tag{11}$$

for the face sheets similar to Equation (3) are introduced, by which the dependence of the equation on x_3 is eliminated. The equation is integrated by parts wherever possible and the terms with equal dependence on the virtual displacements δu_i^{a} and δu_i^{d} are collected. As a result, a single linear homogeneous equation for the virtual displacements is obtained. Since the virtual displacements are arbitrary and independent, the corresponding coefficients must vanish independently.

From the coefficients in the area integral, the equations of motions

$$\begin{aligned}
0 &= N_{11,1}^{\mathrm{a}} + N_{12,2}^{\mathrm{a}} \\
0 &= N_{12,2}^{\mathrm{a}} + N_{22,2}^{\mathrm{a}} \\
0 &= N_{11,1}^{\mathrm{d}} + N_{12,2}^{\mathrm{d}} + \tfrac{1}{t^c} N_{13}^{\mathrm{c}} \\
0 &= N_{12,2}^{\mathrm{d}} + N_{22,2}^{\mathrm{d}} + \tfrac{1}{t^c} N_{23}^{\mathrm{c}} \\
0 &= \tfrac{1}{r_1} N_{11}^{\mathrm{a}} + \tfrac{1}{r_2} N_{22}^{\mathrm{a}} + M_{11,11}^{\mathrm{a}} + 2M_{12,12}^{\mathrm{a}} + M_{22,22}^{\mathrm{a}} \\
&\quad + \tfrac{t^c + t^f}{t^c}\left(N_{13,1}^{\mathrm{c}} + N_{23,2}^{\mathrm{c}}\right) + q_3^{\mathrm{a}*} - \left(m^{\mathrm{f}} + \tfrac{1}{2} m^{\mathrm{c}}\right) \ddot{u}_3^{\mathrm{a}} \\
0 &= \tfrac{1}{r_1} N_{11}^{\mathrm{d}} + \tfrac{1}{r_2} N_{22}^{\mathrm{d}} + M_{11,11}^{\mathrm{d}} + 2M_{12,12}^{\mathrm{d}} + M_{22,22}^{\mathrm{d}} \\
&\quad + N_{33}^{\mathrm{c}} + q_3^{\mathrm{d}*} - \left(m^{\mathrm{f}} + \tfrac{1}{6} m^{\mathrm{c}}\right) \ddot{u}_3^{\mathrm{d}}
\end{aligned} \tag{12}$$

are obtained. In a similar manner, the boundary conditions

$$
\begin{array}{llll}
u_n^{\mathrm{a}} = u_n^{\mathrm{a}*} & \text{or} & N_{nn}^{\mathrm{a}} & = N_{nn}^{\mathrm{a}*} \\
u_t^{\mathrm{a}} = u_t^{\mathrm{a}*} & \text{or} & N_{nt}^{\mathrm{a}} & = N_{nt}^{\mathrm{a}*} \\
u_n^{\mathrm{d}} = u_n^{\mathrm{d}*} & \text{or} & N_{nn}^{\mathrm{d}} & = N_{nn}^{\mathrm{d}*} \\
u_t^{\mathrm{d}} = u_t^{\mathrm{d}*} & \text{or} & N_{nt}^{\mathrm{d}} & = N_{nt}^{\mathrm{d}*} \\
u_3^{\mathrm{a}} = u_3^{\mathrm{a}*} & \text{or} & M_{nn,n}^{\mathrm{a}} + 2M_{nt,t}^{\mathrm{a}} + \frac{t^{\mathrm{c}}+t^{\mathrm{f}}}{t^{\mathrm{c}}} N_{n3}^{\mathrm{c}} & = M_{nt,t}^{\mathrm{a}*} + \frac{1}{2} N_{n3}^{\mathrm{c}*} \\
u_3^{\mathrm{d}} = u_3^{\mathrm{d}*} & \text{or} & M_{nn,n}^{\mathrm{d}} + 2M_{nt,t}^{\mathrm{d}} & = M_{nt,t}^{\mathrm{d}*} + \frac{1}{t^{\mathrm{c}}} M_{n3}^{\mathrm{c}} \\
u_{3,n}^{\mathrm{a}} = u_{3,n}^{\mathrm{a}*} & \text{or} & M_{nn}^{\mathrm{a}} & = M_{nn}^{\mathrm{a}*} \\
u_{3,n}^{\mathrm{d}} = u_{3,n}^{\mathrm{d}*} & \text{or} & M_{nn}^{\mathrm{d}} & = M_{nn}^{\mathrm{d}*}
\end{array}
\tag{13}
$$

follow from the boundary integral. The same equations would be obtained by discarding all geometrically nonlinear terms in the corresponding equations of motion and boundary conditions of the original v. Kármán model (Hohe and Librescu [5], [6]). Notice that so far all equations of the model are independent from the material behaviour of core and face sheets.

2.4 Material Model

In the present study, sandwich panels with laminated, infinite fibre reinforced face sheets and orthotropic cores are considered. The two face sheets are assumed to be identical and symmetric with respect to their individual central surface. Hence, their material response is defined by

$$
\begin{Bmatrix}
\begin{pmatrix} N_{11}^{\mathrm{a}} \\ N_{22}^{\mathrm{a}} \\ N_{12}^{\mathrm{a}} \end{pmatrix}, \begin{pmatrix} N_{11}^{\mathrm{d}} \\ N_{22}^{\mathrm{d}} \\ N_{12}^{\mathrm{d}} \end{pmatrix}
\end{Bmatrix} =
\begin{pmatrix}
A_{11}^{\mathrm{f}} & A_{12}^{\mathrm{f}} & A_{16}^{\mathrm{f}} \\
 & A_{22}^{\mathrm{f}} & A_{26}^{\mathrm{f}} \\
(\mathrm{sym}) & & A_{66}^{\mathrm{f}}
\end{pmatrix}
\begin{Bmatrix}
\begin{pmatrix} \varepsilon_{11}^{\mathrm{a}} \\ \varepsilon_{22}^{\mathrm{a}} \\ 2\varepsilon_{12}^{\mathrm{a}} \end{pmatrix}, \begin{pmatrix} \varepsilon_{11}^{\mathrm{d}} \\ \varepsilon_{22}^{\mathrm{d}} \\ 2\varepsilon_{12}^{\mathrm{d}} \end{pmatrix}
\end{Bmatrix}
\tag{14}
$$

$$
\begin{Bmatrix}
\begin{pmatrix} M_{11}^{\mathrm{a}} \\ M_{22}^{\mathrm{a}} \\ M_{12}^{\mathrm{a}} \end{pmatrix}, \begin{pmatrix} M_{11}^{\mathrm{d}} \\ M_{22}^{\mathrm{d}} \\ M_{12}^{\mathrm{d}} \end{pmatrix}
\end{Bmatrix} =
\begin{pmatrix}
D_{11}^{\mathrm{f}} & D_{12}^{\mathrm{f}} & D_{16}^{\mathrm{f}} \\
 & D_{22}^{\mathrm{f}} & D_{26}^{\mathrm{f}} \\
(\mathrm{sym}) & & D_{66}^{\mathrm{f}}
\end{pmatrix}
\begin{Bmatrix}
\begin{pmatrix} \kappa_{11}^{\mathrm{a}} \\ \kappa_{22}^{\mathrm{a}} \\ \kappa_{12}^{\mathrm{a}} \end{pmatrix}, \begin{pmatrix} \kappa_{11}^{\mathrm{d}} \\ \kappa_{22}^{\mathrm{d}} \\ \kappa_{12}^{\mathrm{d}} \end{pmatrix}
\end{Bmatrix}
$$

in terms of the average and half difference mid-plane strains and curvatures $\varepsilon_{\alpha\beta}{}^{\mathrm{a}}$, $\varepsilon_{\alpha\beta}{}^{\mathrm{d}}$, $\kappa_{\alpha\beta}{}^{\mathrm{a}}$ and $\kappa_{\alpha\beta}{}^{\mathrm{d}}$ respectively. The components of the $A_{ij}{}^{\mathrm{f}}$ and $D_{ij}{}^{\mathrm{f}}$ matrices are determined in the usual manner from the integration of the components of the reduced stiffness matrices of the individual plies of the face sheets.

For the linear elastic, orthotropic core, the material equations are derived in a similar manner. The material response is defined by

$$
\begin{pmatrix} N_{33}^{\mathrm{c}} \\ N_{23}^{\mathrm{c}} \\ N_{13}^{\mathrm{c}} \end{pmatrix} =
\begin{pmatrix} A_{33}^{\mathrm{c}} & 0 & 0 \\ 0 & A_{44}^{\mathrm{f}} & 0 \\ 0 & 0 & A_{55}^{\mathrm{f}} \end{pmatrix}
\begin{pmatrix} \varepsilon_{33}^{\mathrm{c}} \\ \varepsilon_{23}^{\mathrm{c}} \\ \varepsilon_{13}^{\mathrm{c}} \end{pmatrix}
\tag{15}
$$

$$
\begin{pmatrix} M_{33}^{\mathrm{c}} \\ M_{23}^{\mathrm{c}} \\ M_{13}^{\mathrm{c}} \end{pmatrix} =
\begin{pmatrix} D_{33}^{\mathrm{c}} & 0 & 0 \\ 0 & D_{44}^{\mathrm{c}} & 0 \\ 0 & 0 & D_{55}^{\mathrm{c}} \end{pmatrix}
\begin{pmatrix} \kappa_{33}^{\mathrm{c}} \\ \kappa_{23}^{\mathrm{c}} \\ \kappa_{13}^{\mathrm{c}} \end{pmatrix}
$$

where $\varepsilon_{i3}{}^{\mathrm{c}}$ and $\kappa_{i3}{}^{\mathrm{c}}$ are the mid-plane strains and curvatures of the core. The matrix coefficients are determined similar as for the face sheets.

3. Solution Procedure

With the kinematic relations (1) to (5), the material equations (14) and (15), the equations of motion (12) and the boundary conditions (13), a complete set of equations for the dynamic problem of doubly curved sandwich panels is available. Since the problem in general cannot be solved in closed form, a numerical solution procedure is required. In order to be able to perform parametric studies in a numerically efficient manner, the present study employs an extended Galerkin procedure for the solution.

For this purpose, the following considerations are restricted to plane or doubly curved sandwich shells with rectangular projection with edge lengths l_1 and l_2 with respect to the x_1 and x_2-directions. Furthermore, the study is restricted to sandwich shells which are simply supported along all external boundaries. In this case, the form

$$
\begin{aligned}
u_3^{\mathrm{a}} &= w_{\mathrm{mn}}^{\mathrm{a}} \sin\left(\lambda_{\mathrm{m}}^{\mathrm{a}} x_1\right) \sin\left(\mu_{\mathrm{n}}^{\mathrm{a}} x_2\right) \\
u_3^{\mathrm{d}} &= w_{\mathrm{pq}}^{\mathrm{a}} \sin\left(\lambda_{\mathrm{p}}^{\mathrm{d}} x_1\right) \sin\left(\mu_{\mathrm{q}}^{\mathrm{d}} x_2\right)
\end{aligned}
\tag{16}
$$

with

$$
\begin{aligned}
\lambda_{\mathrm{m}}^{\mathrm{a}} &= \frac{m\pi}{l_1}, \quad \mu_{\mathrm{n}}^{\mathrm{a}} = \frac{p\pi}{l_2} \\
\lambda_{\mathrm{p}}^{\mathrm{d}} &= \frac{p\pi}{l_1}, \quad \mu_{\mathrm{q}}^{\mathrm{d}} = \frac{q\pi}{l_2}
\end{aligned}
\tag{17}
$$

is an appropriate assumption for the transverse displacements. In Equations (16) and (17), $w_{\mathrm{mn}}{}^{\mathrm{a}}$ and $w_{\mathrm{pq}}{}^{\mathrm{d}}$ are the modal amplitudes, whereas m, n, p and q are the numbers of sine half waves with respect to the x_1 and x_2-directions for the respective eigenmode of the free vibration.

In the next step, a solution for the in-plane displacements $u_1{}^{\mathrm{a}}$, $u_1{}^{\mathrm{d}}$, $u_2{}^{\mathrm{a}}$ and $u_2{}^{\mathrm{d}}$ is derived, which is consistent with the assumed form (16) and (17) of the transverse displacements. Following the procedure utilized in the previous studies (Hohe and Librescu [5], [6]), the assumptions (16) and (17) are substituted into the first four equations of the set (12) of the equations of motion. By this means, a consistent solution for the unknown displacements is obtained which satisfies the first four equilibrium conditions exactly. The simply supported boundary conditions with respect to the transverse deflections $u_3{}^{\mathrm{a}}$ and $u_3{}^{\mathrm{d}}$ are satisfied identically. All other boundary conditions are satisfied in an integral average sense. The only remaining unknowns are the modal amplitudes $w_{\mathrm{mn}}{}^{\mathrm{a}}$ and $w_{\mathrm{pq}}{}^{\mathrm{d}}$ of the transverse displacements.

Following the concept of the extended Galerkin procedure, the assumption (16) and (17) for the transverse displacements together with a similar assumption for the virtual transverse displacements $\delta w_{\mathrm{mn}}{}^{\mathrm{a}}$ and $\delta w_{\mathrm{pq}}{}^{\mathrm{d}}$ and together with the consistent solution for the in-plane displacements is substituted into Hamilton's principle (6) together with the expressions (7) to (8) for the individual virtual energy terms and the stress resultants (10) and (11). The stress resultants are expressed through the material equations (14) and (15) in terms of the strains and curvatures of the three principal layers which are substituted with the displacement expressions in terms of the modal amplitudes using the kinematic relations (5) together with Equations (1) to (4). As a result a single homogeneous linear equation for the two virtual modal amplitudes $\delta w_{\mathrm{mn}}{}^{\mathrm{a}}$ and $\delta w_{\mathrm{pq}}{}^{\mathrm{d}}$ is obtained. Since the virtual modal amplitudes are arbitrary and independent from each other, the corresponding coefficients must vanish independently, yielding a set of two coupled second order differential equations for the unknown modal amplitudes $w_{\mathrm{mn}}{}^{\mathrm{a}}$ and $w_{\mathrm{pq}}{}^{\mathrm{d}}$ as a function of time. In contrast to previous studies based on a v. Kármán type nonlinear approach

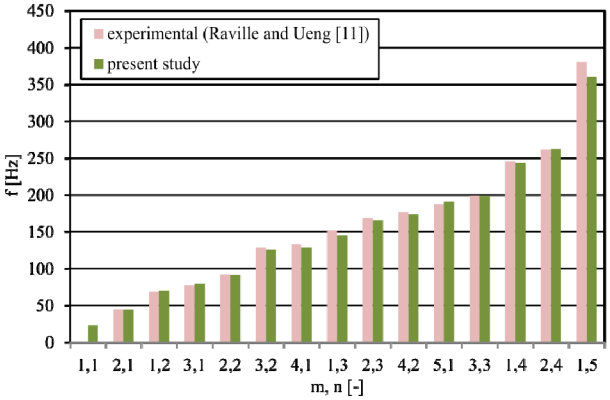

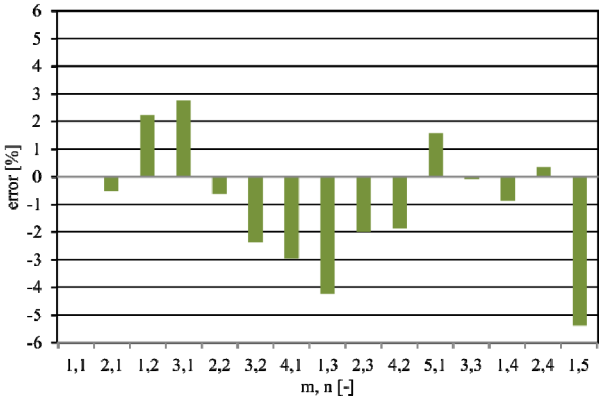

Figure 2. Validation.

(Hohe and Librescu [5], [6]), a much more simple linear system is obtained since all geometrical nonlinearities were discarded in the present study.

The system may be solved as an initial value problem, similar as in preceding studies (e.g. Hohe et al. [7]). In the present study concerning the free vibrations of sandwich structures, a different approach is employed. Assuming harmonic oscillations, the modal amplitudes may be postulated in the form

$$\begin{aligned} w^{a}_{mn} &= \hat{w}^{a}_{mn}\sin(\omega t) \\ w^{d}_{pq} &= \hat{w}^{d}_{pq}\sin(\omega t) \end{aligned} \tag{18}$$

where $\hat{w}_{mn}{}^{a}$ and $\hat{w}_{pq}{}^{d}$ are the amplitudes and ω is a constant. Substituting Equation (18) into the governing system for the amplitudes $w_{mn}{}^{a}$ and $w_{pq}{}^{d}$ constitutes a system of the type

$$\begin{pmatrix} \left(K_{11}+\omega^2\right) & K_{12} \\ K_{21} & \left(K_{22}+\omega^2\right) \end{pmatrix} \begin{pmatrix} \hat{w}^{a}_{mn} \\ w^{d}_{pq} \end{pmatrix} = \begin{pmatrix} 0 \\ 0 \end{pmatrix} \tag{19}$$

where K_{11}, K_{12}, K_{21} and K_{22} are coefficients depending on the geometry and material constants of the sandwich panel as well as on the numbers m, n, p and q of the sine half waves in the eigenmode according to Equation (16). Since the system (19) is linear and homogeneous, non-trivial solutions for the amplitudes $\hat{w}_{mn}{}^{a}$ and $\hat{w}_{pq}{}^{d}$ can only exist, if the determinant of the system matrix vanishes. Hence, the natural frequency

$$f = \frac{\omega}{2\pi} \tag{20}$$

for the mode with the numbers m, n, p and q of sine half waves is determined through the smallest positive solution

$$\omega^2 = -\tfrac{1}{2}\left(K_{11}+K_{22}\right) \pm \left(\tfrac{1}{4}\left(K_{11}-K_{22}\right)^2 + K_{12}K_{21}\right)^{\frac{1}{2}} \tag{21}$$

of the characteristic equation.

4. Examples

4.1 Validation

In a first application, the model is validated against experimental results from literature. In their now classical study, Raville and Ueng [11] have reported measurements of the first natural frequencies for simply supported plane rectangular sandwich plates. The panel consists of isotropic aluminium face sheets bonded to a honeycomb core. The geometry and the material properties are summarized in Table 1.

The experimental results of Raville and Ueng together with the corresponding numerical results obtained by the procedure described in the previous section are presented in Figure 2. For all considered eigenmodes, an almost perfect agreement is obtained. The largest deviation of experimental and numerical data is obtained for the mode with $m = 1$ and $n = 5$ with 5.4%. Hence, the present procedure proves to be accurate.

4.2 Plane Sandwich Plates

To study the effect of core and face sheet anisotropy on the natural frequencies and the corresponding eigenmodes, the structural sandwich model is applied in parametric studies concerning different types of sandwich structures. As a first example, a plane square sandwich plate is considered. The plate is assumed to consist of laminated carbon epoxy face sheets with eight plies in a symmetric $[0°/\pm\vartheta/90°]_s$ stacking sequence. The material data is chosen such that the material is characteristic for a carbon epoxy material with approximately 50% fibre volume fraction as it might be processed by a resin transfer moulding process which becomes increasingly popular for industrial scale applications e.g. in the automotive industry. The core material is chosen in the characteristic range for aluminium honeycomb core with anisotropic transverse shear properties. The geometry and material data chosen as a starting point for the parametric studies is summarized in Table 2.

Table 1. Validation Example (Raville and Ueng [11]).

external geometry			
l_1 [mm]	l_2 [mm]	$1/r_1$ [mm^{-1}]	$1/r_2$ [mm^{-1}]
1828.8	1219.2	0.0	0.0
face sheets (aluminium)			
E [GPa]	ν [-]	t^f [mm]	ρ^f [kg/m^3]
68.948	0.33	0.46	3721
core (honeycomb)			
G_{23} [MPa]	G_{13} [MPa]	t^c[mm]	ρ^c [kg/m^3]
51.7	134.5	6.35	≈ 0

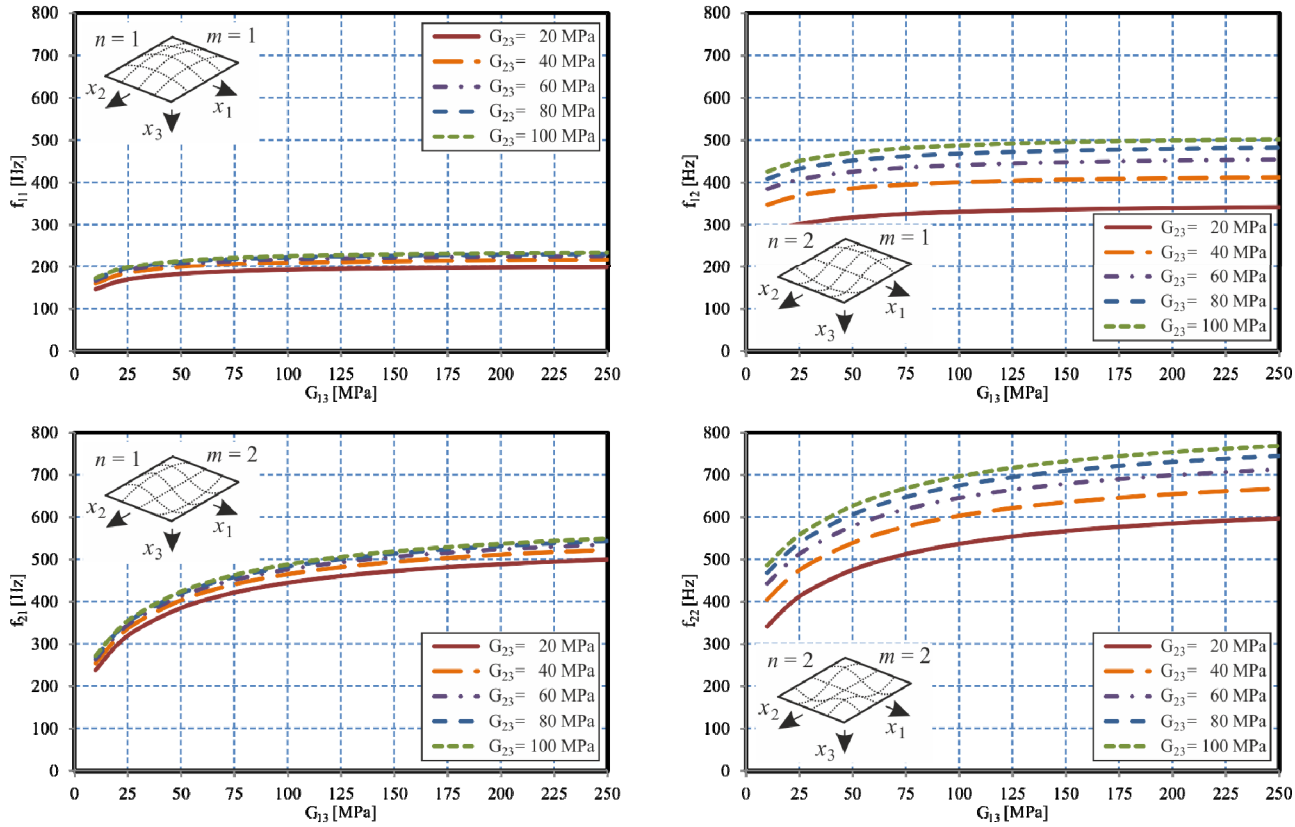

Figure 3. Plane Sandwich Panel – Effect of the Transverse Core Stiffness.

In a first parametric study, the effect of the transverse shear moduli of the core is investigated. For this purpose, the natural frequencies for the eigenmodes with $(m, n) = (1, 1)$, $(m, n) = (1, 2)$, $(m, n) = (2, 1)$ as well as $(m, n) = (2, 2)$ which are assumed to be the leading eigenmodes are computed for a variety of values for the transverse shear moduli G_{23} and G_{13}. The fibre angle ϑ is kept constant at $\vartheta = 45°$ so that the face sheets are quasi-isotropic. All other material and geometry parameters are kept constant at their designated values according to Table 2. The results are presented in Figure 3.

In all modes, a distinct drop in the first natural frequencies is observed in the weak core limit for G_{23}, $G_{13} \to 0$. In this case, the core loses its stiffness so that the limit case of two uncoupled laminated plates is approached. Due to the decreased stiffness, the eigenfrequencies decrease as well. For large transverse shear moduli G_{23} and G_{13}, the increasingly stiff core requires an increasing amount of in-plane stretching and compression of the face sheets, since the increasing transverse core stiffness increasingly constrains the relative lateral displacements of the face sheets whereas in the weak core limit with vanishing transverse core stiffness, the two face sheets may bend with respect to their individual mid-surfaces rather than with respect to the mid-surface of the entire sandwich structure as in the strong core limit.

Table 2. Basic Geometry and Material data for the Parametric Studies.

external geometry			
l_1 [mm]	l_2 [mm]	$1/r_1$ [mm^{-1}]	$1/r_2$ [mm^{-1}]
1000.0	1000.0	0.0	0.0

face sheets (carbon epoxy, $[0°/\pm\vartheta/90°]_s$)					
E_l [GPa]	E_t [GPa]	ν_{lt} [-]	G_{lt} [GPa]	ρ^f [kg/m^3]	t^{ply} [mm]
114.0	10.0	0.34	5.4	1550	0.25

core (aluminium honeycomb)				
G_{23} [MPa]	G_{13} [MPa]	E_3 [MPa]	ρ^c [kg/m^3]	t^c [mm]
186.0	98.6	234.0	50.0	30.0

Depending on the anisotropy of the core, a different order of the four eigenmodes with respect to the corresponding eigenfrequencies develops. In this context, e.g. for $G_{23} = 100$ MPa and small G_{13}, f_{21} is the second natural frequency whereas f_{12} is the third one. For $G_{13} > 100$ MPa and thus $G_{13} > G_{23}$, the two eigenfrequencies exchange their roles and f_{12} becomes the second eigenfrequency whereas f_{21} becomes the third one. Hence, for standard honeycomb cores with non-isotropic transverse shear moduli, care has to be taken with respect to its assembly direction since a rotated assembly of the core might affect the order of the natural frequencies and thus might result in another eigenmode to become the critical one.

In the next parametric study, the effect of the core and face sheet anisotropy is studied in more detail. For this purpose, the fibre angle ϑ is varied over the entire interval $[0°, 90°]$. In this context, $\vartheta = 0°$ constitutes a face sheet layup with six layers orientated towards the x_1-direction and only two layers within the x_2-direction. Hence, for $\vartheta = 0°$, the x_1-direction is the strong direction whereas x_2 is the weaker direction. For $\vartheta = 90°$, the directions exchange their roles. The case $\vartheta = 45°$ constitutes the case of qua-

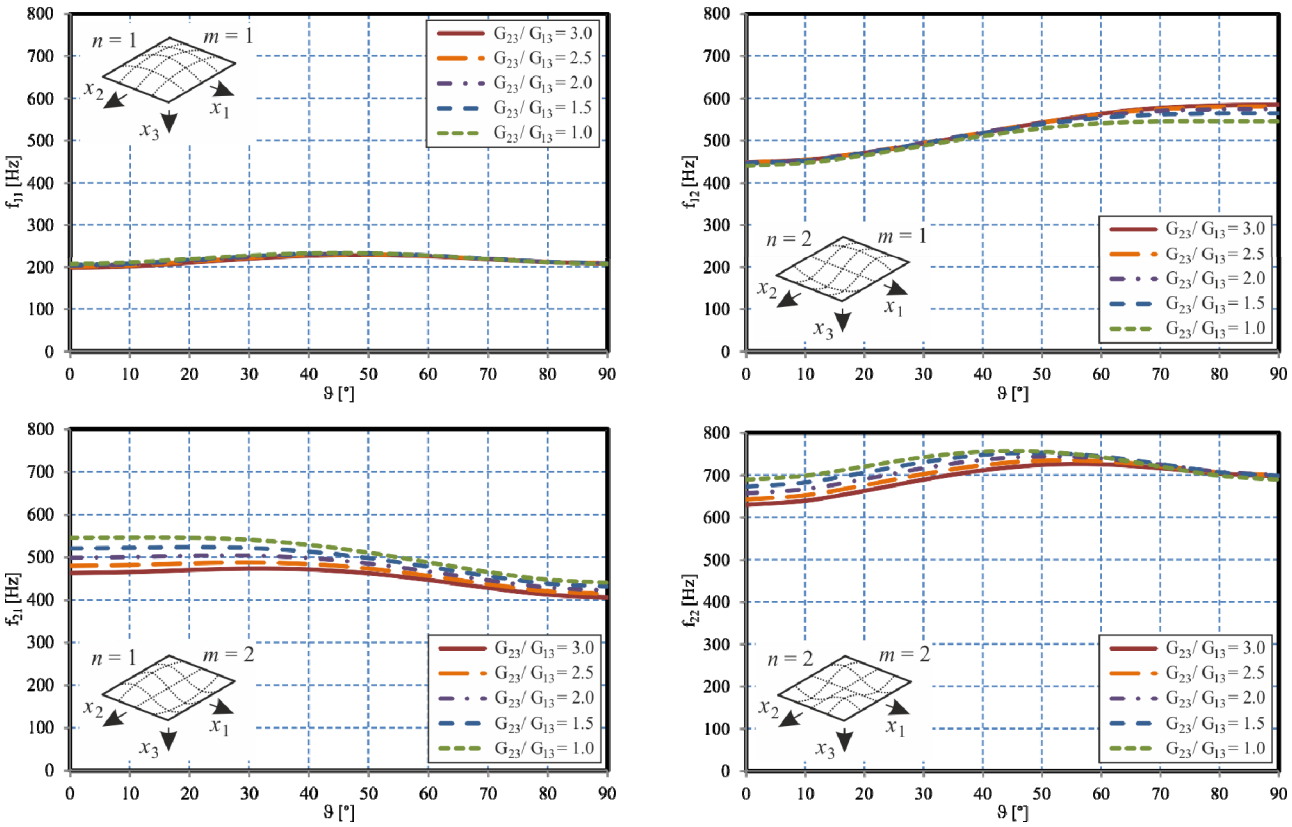

Figure 4. Plane Sandwich Panel – Effect of the Core and Face Sheet Anisotropy.

si-isotropic face sheets. Five different ratios G_{23}/G_{13} for the transverse shear moduli are considered, where the two shear moduli are chosen such that the average transverse shear modulus is $(G_{23} + G_{13})/2 = 140$ MPa. Again, a plane sandwich plate with all other properties according to Table 2 is considered.

The results are presented in Figure 4. For the first eigenmode corresponding to the natural frequency f_{11}, only minor effects of the anisotropy of the core and the face sheets are observed. The eigenfrequency f_{12} increases with increasing fibre angle ϑ and thus increasing stiffness within the x_2-direction forming the direction with two sine half waves (and thus the direction with the shorter modal wave length). The opposite effect is observed for the eigenfrequency f_{21}, since in this case, the number of modal waves within the x_1- and x_2-directions have been exchanged. Due to the core anisotropy the curves for these two eigenmodes are not obtained as mirror image of each other, except for the case $G_{23}/G_{13} = 1$, when the core becomes isotropic. Again, it is observed that the natural frequencies f_{12} and f_{21} exchange their order depending on the core and face sheet anisotropy. Hence, care has to be taken in an optimization of the laminate stacking sequences for an improvement of either the stiffness or static strength of the structure, since a variation in the anisotropy of the structure – although possibly advantageous for the static response – might have disadvantageous effects on the dynamic response. Especially, eigenmodes, which were initially non critical might become the leading ones.

The effect of the core anisotropy on the natural frequencies depends on the eigenmode considered. As it can be observed in Figure 4, the core anisotropy ratio G_{23}/G_{13} has a stronger influence on the eigenfrequencies for the two modes with $m = 2$, compared to the other two modes. Since in the current parametric study, G_{23} is larger than G_{13} (except for $G_{23}/G_{13} = 1$), the x_2-direction is the direction supplied with an increasing stiffness with increasing deviation of the anisotropy ratio from $G_{23}/G_{13} = 1$. On the other hand, compared to the modes with $m = 1$, the eigenmodes with $m = 2$ feature a shorter modal wave length within the x_2-direction. Thus, an increasing core shear stiffness towards this direction results in an increasingly constrained deformation, causing the stronger effects of G_{23}/G_{13} observed in Figure 4 for f_{21} and f_{22}.

4.3 Curved Sandwich Shells

In further parametric studies, the effect of the anisotropy of the honeycomb core and the composite face sheets on curved sandwich structures is investigated. Both, cylindrical sandwich shells with either $\rho_1 = 1/r_1 \neq 0$ or $\rho_2 = 1/r_2 \neq 0$ (and the other radius equal to zero) and doubly curved sandwich shells with both $\rho_1 \neq 0$ and $\rho_2 \neq 0$ are analysed.

In a first study, the effect of the curvature on the natural frequencies is investigated. As an example, a sandwich shell with square projection, quasi-isotropic laminated faces and honeycomb core according to Table 1 is considered. The curvatures ρ_i are varied over the interval [-1 m^{-1}, 1 m^{-1}]. The results for the first four eigenmodes are presented in Figure 5. Figure 6 gives a sketch on the geometry ranges considered.

In general, a strong effect of the curvature radii on the natural frequencies is observed, since the curvature of the

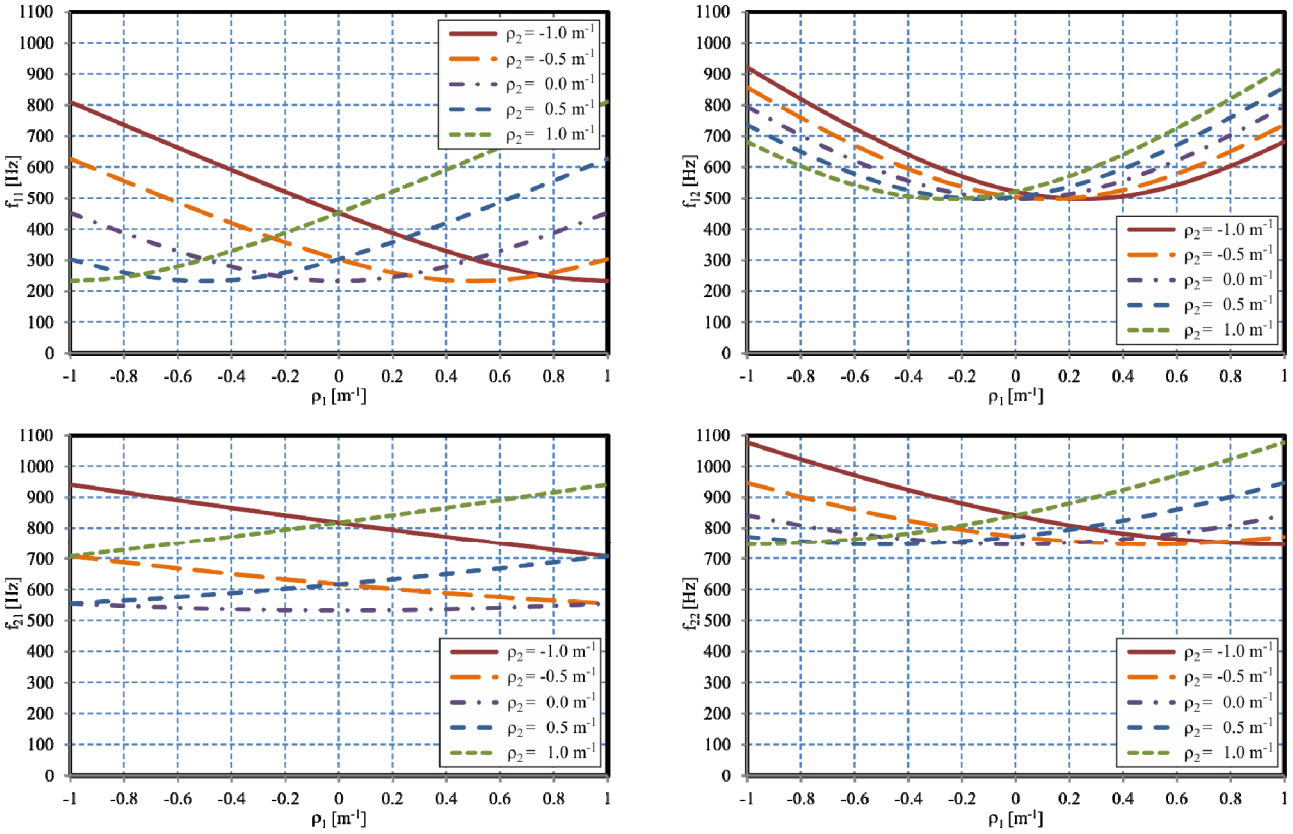

Figure 5. Doubly Curved Sandwich Shell – Effect of the Curvature.

structures strongly influences their (structural) stiffness. The spherical sandwich cap with $\rho_1 = \rho_2$ features the strongest structural stiffness. Hence, large eigenfrequencies for all eigenmodes are obtained especially in these cases. Decreasing natural frequencies are obtained, when the geometry approaches the cylindrical case with either $\rho_1 = 0$ or $\rho_2 = 0$. Further decreases are obtained in the limit of the plane sandwich plate with $\rho_1 = \rho_2 \rightarrow 0$. Nevertheless, for the first natural frequency f_{11}, similar values as for the plane plate are obtained for sandwich saddle shells with $\rho_1 = -\rho_2$.

Due to the core anisotropy with G_{23} G_{13} (see Table 2), the results for f_{12} and f_{21} are dissimilar despite the symmetry of the external geometry of the structures under consideration. It is observed that the order of the eigenfrequencies especially for these two eigenmodes depends on the ratio ρ_1/ρ_2 of the curvatures, since different curvatures constitute a different structural stiffness with respect to the two spatial directions x_1 and x_2 and thus different (structural) constraints on the respective deformation.

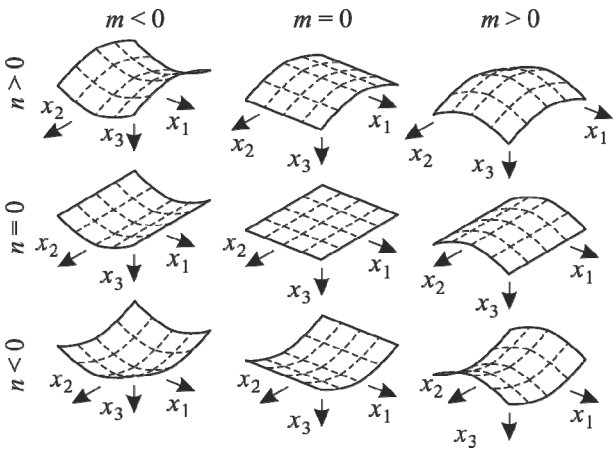

Figure 6. Doubly Curved Geometries.

In order to study the effect of the anisotropy of the honeycomb core and the laminated composite face sheets in more detail, similar parameter studies as in Figure 4 for the case of a plane sandwich plate are performed for the cases of a cylindrical sandwich shell with $\rho_1 = 1\ m^{-1}$ and $\rho_2 = 0$, a spherical sandwich cap with $\rho_1 = \rho_2 = 1\ m^{-1}$ as well as for a sandwich saddle structure with $\rho_1 = -\rho_2 = 1\ m^{-1}$. As before, the fibre angle ϑ is varied over the interval [0°, 90°] considering five different core shear stiffness ratios G_{23}/G_{13} with an average of $(G_{23} + G_{13})/2 = 140$ MPa. All other parameters are kept constant at the values compiled in Table 2. The results are presented in Figures 7, 8 and 9 respectively.

For the cylindrical sandwich shell (Figure 7), qualitatively similar effects of the core shear stiffness anisotropy ratio G_{23}/G_{13} are obtained. Whereas, only rather weak effects are observed for the natural frequencies f_{11} and f_{12}, moderate effects are obtained on f_{21} and f_{22}, since these two modes involve a shorter modal wave length within the x_2-direction as the stronger direction for $G_{23}/G_{13} > 1$.

Due to the non-zero curvature ρ_1 within the x_1-direction, especially the eigenmodes for f_{11} and f_{12}, i.e. those modes involving only a single modal wave within the x_1-direction are stronger constrained than in the case of the plane sandwich plate in Figure 2. As a consequence, higher natural frequencies f_{11} and f_{12} are obtained for the cylindrical sandwich shell, compared to the plane sandwich plate. The nat-

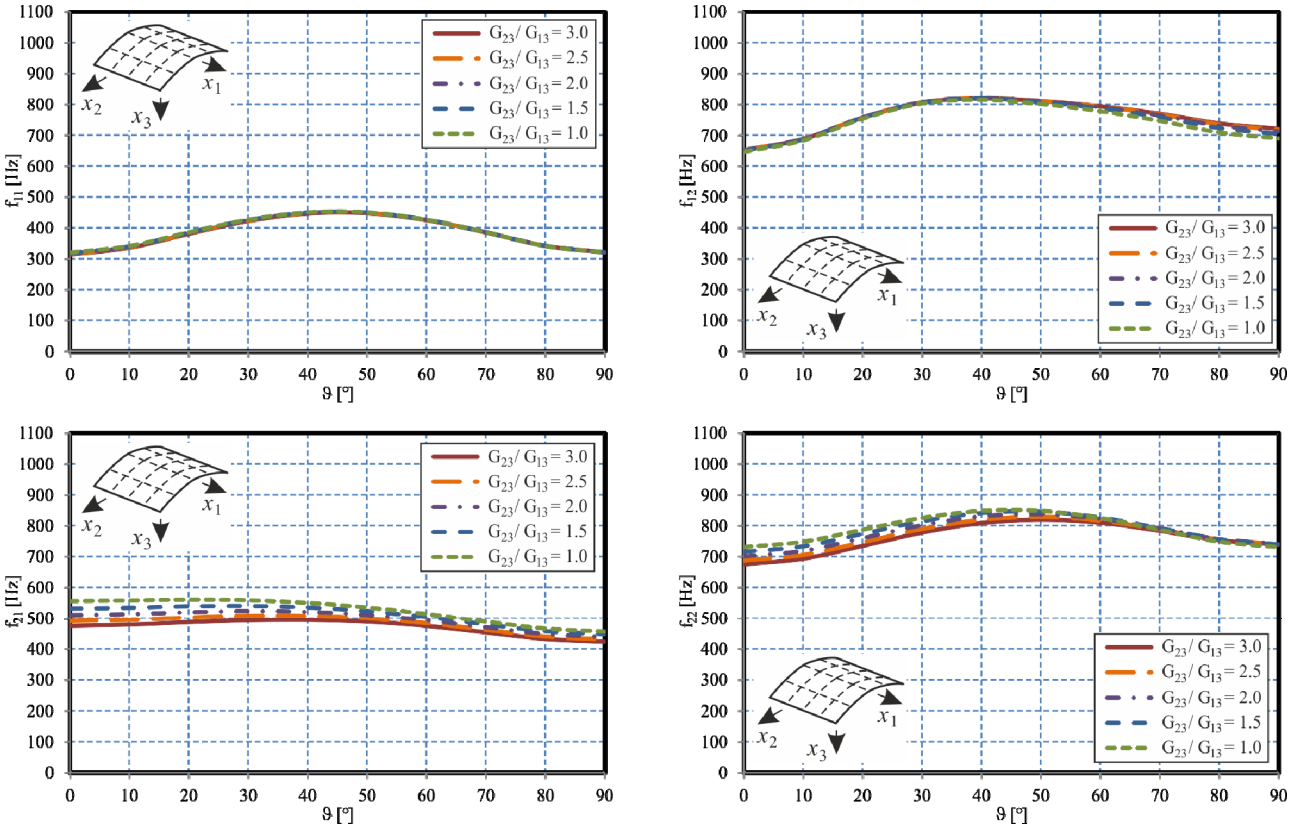

Figure 7. Cylindrical Sandwich Shell – Effect of Core and Face Sheet Anisotropy.

ural frequencies f_{21} and f_{22} are also slightly higher than for the plane plate, nevertheless, the effect is less distinct.

Cross-relation effects between the structural stiffness increase due to the shell curvature and stiffness variations due to the varying anisotropy of the core and face sheet material cause a qualitatively different characteristics of the individ-

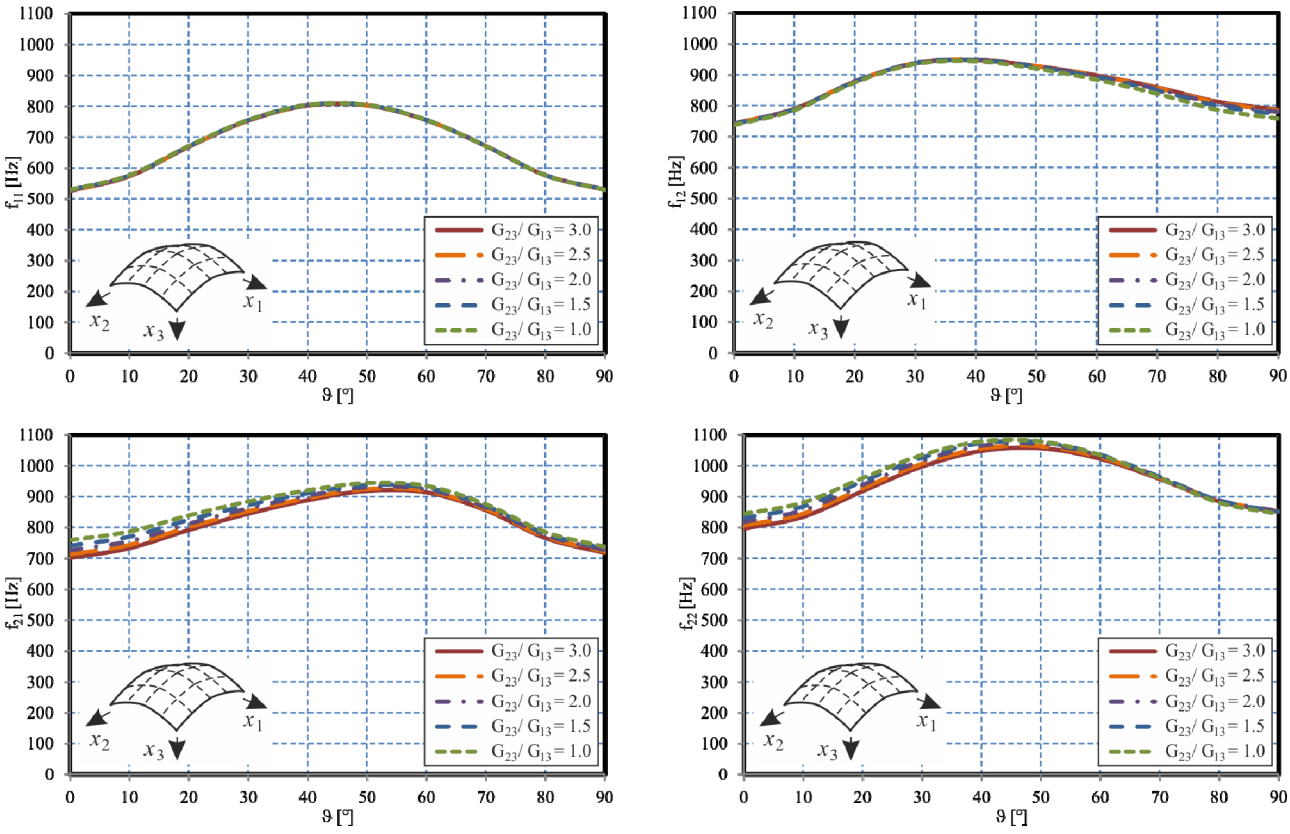

Figure 8. Spherical Sandwich Cap – Effect of the Curvature.

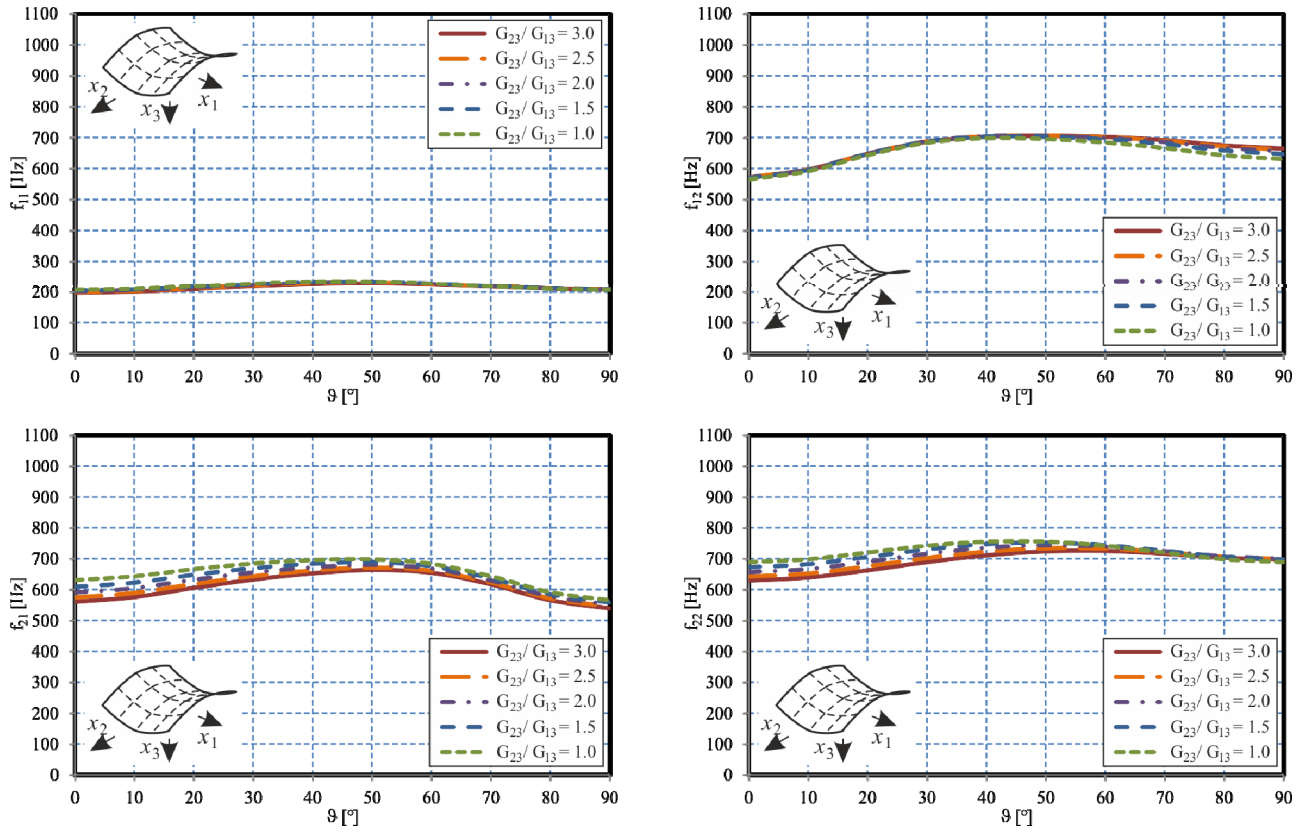

Figure 9. Sandwich Saddle Shell – Effect of Core and Face Sheet Anisotropy.

ual curves for the cylindrical shell compared to the plane plate. Effects are observed especially for the natural frequency f_{12}. In this context, the asymmetric curves for $f_{12}(\vartheta)$ is caused by the uniaxial curvature of the shell. Another effect of the additional structural stiffness of the cylindrical effect is the fact that in part of the considered range for the fibre angle ϑ and the core shear stiffness ratio G_{23}/G_{13}, the natural frequency f_{22} is found below the natural frequency f_{12} (i.e. $\vartheta \approx 30°$, G_{23}/G_{13} 2, see Figure 7). In this case, f_{11}, f_{21}, f_{22} and f_{12} are the first, second, third and fourth eigenfrequency, respectively. In general, more distinct effects of the face sheet anisotropy through the fibre angle ϑ are observed.

Even stronger effects of the fibre angle ϑ on all four eigenmodes considered in the present study are observed for the doubly curved spherical sandwich cap investigated in Figure 8. For f_{11}, f_{12} and f_{22} qualitatively similar results as in the case of the cylindrical sandwich shell are obtained. For the natural frequency f_{21}, a similar dependence on the fibre angle J is obtained as for f_{12} due to the double curvature of the sandwich cap. For the case of an isotropic core with $G_{23}/G_{13} = 1$, the dependencies of the natural frequencies f_{12} and f_{21} are mirror images of each other with respect to the case $\vartheta = 45°$, i.e. the case of complete isotropy of both, the core and the face sheet material. For other core anisotropy ratios G_{23}/G_{13} the curves for $f_{12}(\vartheta)$ and $f_{21}(\vartheta)$ respectively are not obtained as mirror images of the respective other curve due to the anisotropy of the core for G_{23}/G_{13} 1.

In a final parametric study, the case of a saddle type sandwich shell is considered as an example for a doubly curved sandwich shell with anticlastic curvature rather than synclastic curvature as in the case of the spherical sandwich cap. The results are compiled in Figure 9. For the natural frequencies f_{11} and f_{22} as the eigenfrequencies with similar numbers of $m = n$ of modal waves with respect to the x_1- and x_2-directions, values rather close to the corresponding values for the plane sandwich plate are obtained (see Figures 4 and 9). For these two modes, the anticlastic curvature of the structure with $\rho_1 = -\rho_2$ obviously does not constitute a distinct increase in structural stiffness. For the two eigenmodes with m n, even the anticlastic curvature increasingly constrains the deformation compared to the case of a plane sandwich plate. As a consequence, the corresponding natural frequencies f_{12} and f_{21} are larger than in the case of the plane plate. Nevertheless, even f_{12} and f_{21} are found below the corresponding natural frequencies for the sandwich cap with synclastic curvature. In general, the effect of the anisotropy of the honeycomb core and the laminated face sheets has less distinct effects than for the sandwich cap.

5. Conclusions

The present study is concerned with a numerical analysis of the effect of the anisotropy of core and composite face sheets on the free vibration of plane and curved sandwich plates and shells. For the analysis, a simplified, geometrically linear reformulation of a previous, more general sandwich shell theory is utilized. The model is based on the Kirchhoff-Love model for the face sheets and a second/first order power-series expansion of the core displacements.

Consistent equations of motion and boundary conditions are derived by means of Hamilton's variational principle.

For the case of simply supported sandwich plates or shells with rectangular projection, an analytical solution is derived by means of an extended Galerkin procedure. Assuming harmonic oscillations, an eigenvalue problem is obtained, governing the natural frequencies. In a validation against experimental data from literature, the model proves to be accurate and numerically extremely efficient, making it a powerful tool for a fast execution of parametric studies concerning the natural frequencies and corresponding eigenmodes of the considered class of sandwich structures.

The model is applied in parametric studies regarding the effect of fibre angles of the composite laminated face sheets and the anisotropy in the transverse shear moduli of the core on the lower natural frequencies of sandwich structures. It is observed that the natural frequencies are affected in a complex combined manner by structural stiffness effects due to the shell curvatures together with the anisotropy in the material stiffness of the principal layers. It is observe that the leading eigenmodes of the free vibration might distinctively be affected by variations in the composite design such as variation in the composite lay-up, fibre angles and assembly angle of an anisotropic honeycomb core. The significance of the effect depends in a complicated manner on the interactions of structural stiffness induced e.g. by panel curvatures and the material stiffness distribution. Hence, care has to be taken when optimizing the composite stacking sequence and fibre angles for the objective of overall static stiffness and strength, since variations in the composite material design may affect the first natural frequencies and may even result in changes in the leading critical eigenmodes.

REFERENCES

[1] Bardell, N.S., Dunsdon, J.M. and Langley, R.S., 1997, Free vibration analysis of coplanar sandwich panels, Composite Structures, 38, 463-475.

[2] Frostig, Y. and Thomsen, O.T., 2004, High-order free vibration of sandwich panels with a flexible core, International Journal of Solids and Structures, 41, 1697-1724.

[3] Gibson, L.J. and Ashby, M.F., 1997, Cellular solids – structure and properties, Cambridge University Press, Cambridge.

[4] Hause, T. and Librescu, L., 2006, Flexural free vibration of sandwich flat panels with laminated anisotropic face sheets, Journal of Sound and Vibration, 297, 823-841.

[5] Hohe, J. and Librescu, L., 2003, A nonlinear theory for doubly curved anisotropic sandwich shells with transversely compressible core, International Journal of Solids and Structures, 40, 1059-1088.

[6] Hohe, J. and Librescu, L., 2004, Core and face-sheet anisotropy in deformation and buckling of sandwich panels, AIAA Journal, 42, 149-158.

[7] Hohe, J., Librescu, L. and Oh, S.Y., 2006, Dynamic buckling of flat and curved sandwich panels with transversely compressible core, Composite Structures, 74, 10-24.

[8] Kant, T. and Swaminathan, K., 2001, Analytical solutions for free vibration of laminated composite and sandwich plates based on a higher-order refined theory, Composite Structures, 53, 73-85.

[9] Meunier, M. and Shenoi, R.A., 2001, Dynamic analysis of composite sandwich plates with damping modelled using high-order shear deformation theory, Composite Structures, 54, 243-254.

[10] Nayak, A.K., Moy, S.S.J. and Shenoi, R.A., 2002, Free vibration analysis of composite sandwich plates based on Reddy's higher-order theory, Composites B, 33, 505-519.

[11] Raville, M.E. and Ueng, C.E.S., 1967, Determination of natural frequencies of vibration of a sandwich plate, Experimental Mechanics, 7, 490-493.

[12] Sokolinsky, V.S., Nutt, S.R. and Frostig, Y., 2002, Boundary condition effects in free vibrations of higher-order soft sandwich beams, AIAA Journal 40, 1220-1227.

[13] Vinson, J.R., 1999, The behavior of sandwich structures of isotropic and composite materials, Technomic Publishing, Lancaster, PA.

[14] Yuan, W.X. and Dawe, D.J., 2002, Free vibration of sandwich plates with laminated faces, International Journal for Numerical Methods in Engineering 54, 195-217.

[15] Yuan, W.X. and Dawe, D.J., 2004, Free vibration and stability analysis of stiffened sandwich plates, Composite Structures, 63, 123-137.

[16] Zenkert, D., 1997, An introduction to sandwich construction, EMAS Publishing, Warley.

[17] Zhou, H.B. and Li, G.Y., 1996, Free vibration analysis of sandwich plates with laminated faces using spline finite point method, Computers & Structures, 59, 257-263.